International Journal of Scientific Engineering and Research (IJSER)
ISSN (Online): 2347-3878
Impact Factor (2024): 7.741

Crystal Field Analysis of the Magnetic Anisotropy of $CeAgAs_2$

A. Elhag[1], K. Ayuel[2], A. Al-Qarni[3]

[1]Physics Department, College of Science, Qassim University, Qassim, Saudi Arabia
Correspondence Author Email: *af.alhg[at]qu.edu.sa*
ahmedalhaj65[at]gmail.com
Tel.: +966 541372075

[2]Department of Physics, Al - Baha University, P. O. Box (1998), Saudi Arabia

[3] Physics Department, College of Science, Qassim University, Qassim, Saudi Arabia

Abstract: ***We have investigated the effect of crystal field potential together with the Ce - Ce exchange interaction on the magnetic anisotropy energy, magnetization, and magnetic susceptibility of the Kondo compound $CeAgAs_2$. The effective Hamiltonian for the Ce^{3+} ion was approximated by assuming a tetragonal crystal field, for which the crystal field parameters are estimated using a maximally localized Wannier function approximation, while the exchange part is approximated by mean field approach. Energy eigenvalues and eigenvectors of the magnetic ion in the structure (Ce^{3+}) are determined by diagonalizing the effective Hamiltonian and hence used to estimate the direction - dependent free energy. The magnetocrystalline anisotropy energy was extracted as well as magnetization and magnetic susceptibility in the principal crystallographic axes. Our results reveal that the c - axis is the hard direction of magnetization, while the ab plane is clearly the easy plane, in qualitative agreement with the experimental findings of previous investigations.***

Keywords: Magnetocrystalline anisotropy, $CeAgAs_2$, Crystal field. Mean field approximation

1. Introduction

Kondo lattice compounds of the form $HfCuSi_2$ have been subjected to extensive research effort in condensed matter physics, as it has resulted in the discovery of an abundance of phenomena such as valence fluctuation, quantum phase transition, and heavy fermion [1].

The interplay between the Ruderman, Kittel, Kasuya, and Yosida (RKKY) interactions and the Kondo effect in Ce - based intermetallic compounds was the major subject of investigations, as it underlies interesting phenomena in Ce - based compounds [2].

The magnetism of an intermetallic compound depends on two major effects: the crystalline electric field (CEF) and hybridization between 4f and conduction electrons. A weak hybridization between localized Ce 4f - electrons and the conduction electron should result in a magnetic ground state, while a strong one should give rise to a non - magnetic state as a result of taking the 4f - electron to an intermediate ground state. Both crystal electric field and hybridization depend on the atomic environment around the Ce atoms, where the Ce atom occupies a unique atomic position in the unit cell for most Ce - based compounds. Some Ce intermetallic compounds have two or more crystallographic sites for the cerium atom, which results in different hybridization strengths and different strengths of RKKY exchange interaction, resulting in different degrees of localization for Ce atoms occupying different atomic sites [3].

Myers et. al. have reported that compounds of the form $RAgSb_2$ (R=Y, La - Nd, Sm, and Gd - Tm) have generally shown strong magnetic anisotropy due to CF splitting of ground states of R atoms with a magnetic moment lying in the basal plane and additional anisotropy within the basal plane for $DyAgSb_2$ [4]. As reported by Demchyna et al. and afterwards by Eschen et. al., compounds of the form $HfCuSi_2$ crystallize in a tetragonal unit cell (space group *P4/nmm* No.129) [5, 6], with the Ce atom occupying a unique *2c* position. An XRD investigation conducted by Mondal et. al. [2] has revealed that $CeAgAs_2$ crystallizes in an orthorhombic type of crystal structure (space group *Pmca* No.57), which is connected to the $HfCuSi_2$ tetragonal structure by the relations $\sqrt{2}a_T$ and $2c_T$, with Ce atoms occupying two distinct *4d* Wycoff positions. The symmetry inequivalence is assumed to underlie some interesting properties.

Early reports show that $CeAgAs_2$ orders antiferromagnetically at Neel's temperature (T_N) of 5.5 K; two AFM - like transitions were subsequently observed at Tn = 4.8 K and 6 K, with a magnetic moment of 1 μ_B confined to the basal plane *ab* of the unit cell [7]. The existence of two AFM transitions was asserted by Mondal et al. [2], but most recent investigations conducted by Szlawska et. al. [8] have shown a slightly different result, which is that the AFM ordering below occurs at Tn = 5.5 K while the metamagnetic (MM) transition occurs at an external field of 0.3 T. The study has also shown that magnetic properties are hardly anisotropic throughout the *ab* - plane due to the very slight deviation of the compound structure from tetragonal symmetry.

Despite the abundant literature on magnetic properties of $CeAgAs_2$ amongst other compounds of the same family, our survey of previous investigation has not revealed a theoretical study on these compounds based on a theoretical model that basically combines CF and mean field approximation. On the other hand, a few studies have tackled the important aspect of MAE from a theoretical point of view. In endeavor to establish and test a theoretical model that may successfully account for MAE and subsequently other magnetic properties of RE - based compounds, we have adopted an approach based on the

combined effect of the crystal field interaction and the mean field approximated exchange interaction exhibited by f - electrons of Ce atoms to account for the MCA for the structure - optimized unit cell of $CeAgAs_2$, where the determination of the CF parameters was based on maximally localized Wannier functions (MLWF) approximation. The rest of this paper is organized as follows: in Section 2, we give a brief account of the theoretical method used for calculation, while the results are presented and discussed in Section 3. The conclusion is presented in Section 4.

2. Method

2.1 Crystallographic Structure and CFP's

In order to determine the optimum crystallographic structure and magnetic phase, we have carried out DFT - based first principles calculations on an orthorhombic unit cell of $CeAgAs_2$. In our calculation, we used the full potential linearized augmented plane wave method (FPLAPW) as implemented in the Vienna Ab - initio Simulation Package (WEIN2K) [9]. To treat the electron exchange and correlation, we have employed the PBE - sol generalized gradient approximation (GGA) parameterized by Perdew - Burke and Ernzerhof [10]. The total number of plane waves employed in the calculation was determined by taking the limit of $R_{MT} * K_{max} = 8.0$ (R_{MT} being the muffin - tin sphere radius, and *Kmax* is the maximum amplitude of the lattice vector taken for a plane wave). For all calculations, a k - space mesh of 12×12×6 k - points were used throughout the reduced Brillouin zone. The self - consistent cycle is considered convergent when the total energy of the material is stable within 1.0×10^{-4} Ry. Energy minimization versus unit cell volume was carried out for both FM and AFM configurations of Ce^{3+} ions. SCF calculations were repeated for the minimized crystal structure to determine the Ce 4f energy bands, wherein the Hamiltonian is then expressed in terms of the Wannier basis, particularly maximally localized Wannier functions (MLWF), from which we could extract the on - site CF Hamiltonian. To complete the last step, we have combined the WIEN2WANNIER [11] and the WANNIER90 [12] software packages.

2.2 The effective Hamiltonian:

The effective Hamiltonian, including CF and exchange effects, can be written as

$$H = H_0 + H_{CF} + H_{ex} + H_{Ze} \quad (1)$$

where H_{CF} is the CF interaction Hamiltonian given by the form [13]:

$$H_{CF} = \sum_{kq} B_{kq} \hat{O}_k^q \quad (2)$$

Here B_{kq} are the crystal field parameters (CFP's), usually derived from neutron scattering or magnetic susceptibility data, and $\hat{O}_k^q$ represent the corresponding Stevens' operator equivalents. Assuming magnetization in the crystallographic c - direction (z - axis), the operator equivalents $\hat{O}_k^q$ may be expressed in terms of the polar angle θ and the azimuthal angle φ [14] (see **Appendix A**).

The term H_{ex} in equation (1) is the part indicating the exchange interaction between neighboring Ce - atoms. This term is approximated using the mean field approach as

$$H_{ex} = 2|g-1|\mu_B B_{ex} M_J \quad (3)$$

Where g is the Lande g - factor, μ_B is the Bohr magneton, and $B_{ex}$is the mean external field due to equivalent z nearest neighbors Ce atoms, which is an estimate for the exchange integral as

$$H_{ex} = -2\sum_{i>j} I_{ex}(\boldsymbol{R}_i - \boldsymbol{R}_j)\boldsymbol{S}_i \cdot \boldsymbol{S}_j \quad (4)$$

and, for the i^{th} Ce - atom,

$$H_{ex} = g\mu_B \boldsymbol{B}_{ex} \cdot \boldsymbol{S}_i \quad (5)$$

The $\boldsymbol{B}_{ex}$ is estimated by

$$\boldsymbol{B}_{ex} = \frac{I_{ex}}{g\mu_B}\sum_{j=1}^{z} \boldsymbol{S}_j \quad (6)$$

In terms of the exchange integral, the Curie's temperature T_c can be written as

$$T_c = \frac{2zI_{ex}S(S+1)}{3k} \quad (7)$$

where k is the Boltzmann constant. For the compound under investigation. Following the approach adopted by Endichi et. al [15], we can identify two distinct sets of nearest neighbors, so equation (7) can be rewritten in the form

$$T_c = \frac{2(z_1 I_1 + z_2 I_2) S(S+1)}{3k} \quad (8)$$

where z_k and I_k are the nearest neighbor number and the exchange integral for the *k - th* set of nearest neighbors.

The fourth term in the LHS of equation (1) represents the Zeeman interaction which represents the response to external magnetic field.

2.3 Magnetocrystalline anisotropy energy

A major source of anisotropy energy in rare earth permanent magnets is the magnetocrystalline single - ion anisotropy sublattice. Considering a uniaxial ferromagnetic crystal, for the Ce - ion site being tetragonal in $CeAgAs_2$, the magnetocrystalline anisotropy energy (MAE) per unit volume can be expanded in powers of magnetization direction cosines according to the relation [16]:

$$\frac{E_a}{V} = K_1 sin^2\theta + K_2 sin^4\theta + K_3 sin^4\theta cos4\varphi \quad (9)$$

where the parameters K_i are called the anisotropy constants. Concerning the physical origin of MCA, we can distinguish between several mechanisms responsible for magnetic anisotropy; one is of classical origin based on the multipole (mainly dipole) interactions between momenta localized at lattice points [16]. The second is related to the interaction between the charge density multipoles of a given shell and the crystal field. This term is of electrostatic character, referred to as the

magnetoelectric anisotropy, and is therefore often separated out and treated as a crystal field effect for localized shells (e. g., the 4f - shell in rare earths). The third of these mechanisms is the one considered responsible for magnetocrystalline anisotropy in most modern rare earth magnets. It is mainly a combined effect of the crystalline electric field, the spin orbit coupling, and the intra - atomic exchange. According to this mechanism, the orbital motion of the magnetic electrons is subjected to the electrostatic crystal field due to all the other electrons and nuclei in the crystal. [17]

The crystal field interaction is then transformed into anisotropy energy via the communication of the exchange - coupled spins with the orbital motion of the electron; this is realized by spin - orbit coupling. The calculation of the magnetoelectric energy is based on the Hamiltonian given by equation (1). In some rare earth compounds (e. g., SmCo5), the high anisotropy is thought to stem from the interplay between spin - orbit coupling and the crystal field interaction [17]. This means that the strong spin - orbit coupling tries to align the rare earth *4f* - electron shell with the magnetic field while *4f* - shell electrons in a crystal interact with the crystal field, and the interaction energy depends on the orientation of the 4f - shell in the lattice. If the crystal field is too small in comparison with the spin - orbit coupling, the 4f - shell rotates freely with the magnetic field, producing no magnetic anisotropy energy (MAE). On the other hand, if the spin - orbit coupling is too small, the orbital momentum is quenched, and again, no MAE appears. In view of the above considerations, it is convenient to assume a localized 4f shell subjected to some cubic crystal field comparable in magnitude to the spin orbit coupling, so we shall adopt the second mechanism, and instead of considering the 4f charge density distribution to be either oblate or prolate, we assume the tetragonal symmetry pattern of charge distribution obtained in Sec.3.2.

3. Result and discussion

3.1 Structural Properties and Crystal Fields:

Fig 1. a shows a tetragonal crystal stature of $CeAgAs_2$ with space group P4nm. Fig 1. b displays energy per unit cell volume for FM and AFM phases. This Figure reveals that the ground state energetically favors AFM ground state. Table 1 the refined lattice parameters were tabulated in column 2.

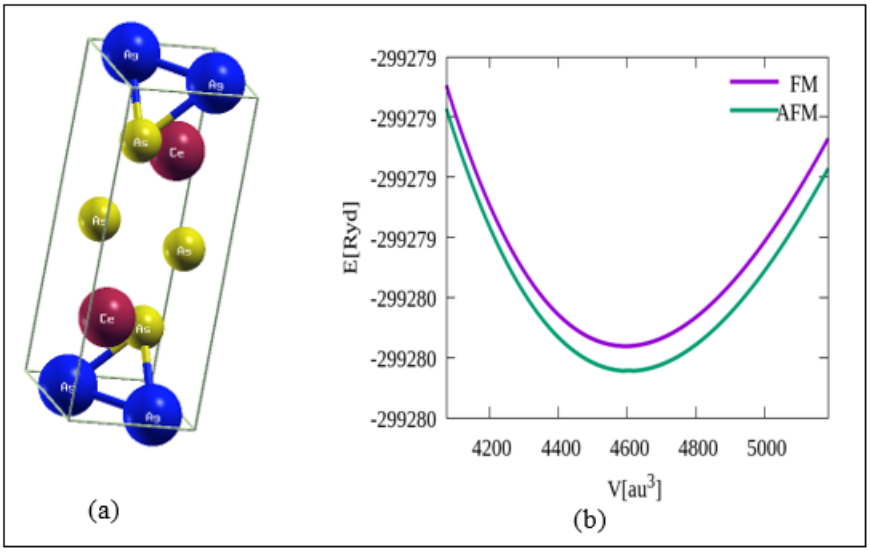

Figure 1: (a) Optimized Tetragonal structure of $CeAgAs_2$ unit cell. (b) Energy vs Unit cell volume for $CeAgAs_2$ crystal.

Table 1: Crystal lattice and CF parameters of $CeAgAs_2$.

Parameter	MLWF Current	Exp. [2]
a (Å)	5.7295	5.7441
b (Å)	5.7351	5.7696
c (Å)	20.983	21.0074
B_2^0 (K)	6.022	5.79
B_2^2 (K)	- 1.571	−2.49
B_4^0 (K)	- 1.192	−2.40
B_4^2 (K)	- 2.005	−1.18
B_4^4 (K)	1.367	1.74

Table.1 shows a qualitatively good agreement of current results of CFP's with experimental results obtained by Mondal et al. [2] in the sense that, the currently used model based on MLWF and ab initio calculations could reproduce the same signs for all CFP's up to fourth order. There is a relatively large discrepancy between fourth - order values. However, fourth - order terms have less effect on the accuracy of CF field - based calculations. The eigenvalues and corresponding eigenstates are obtained by diagonalizing the CF Hamiltonian; the results are shown in Table.2. Where the ground state energy was found to be - 341.689 K in agreement with shifted eigenvalues of energy obtained by Modal. et. al., where the ground state is fixed to 0. This value corresponds to the 2 - fold degenerate G_7 irreducible representation of the Ce site point group C_{2h}.

Table 2: CF ground states and energy eigenvalues of $CeAgAs_2$.

Eigenvalue	Eigen state $\lvert JM_j\rangle$					
E (K)	$\lvert\frac{5}{2}\frac{5}{2}\rangle$	$\lvert\frac{5}{2}\frac{3}{2}\rangle$	$\lvert\frac{5}{2}\frac{1}{2}\rangle$	$\lvert\frac{5}{2}-\frac{1}{2}\rangle$	$\lvert\frac{5}{2}-\frac{3}{2}\rangle$	$\lvert\frac{5}{2}-\frac{5}{2}\rangle$
424.837	0.08919	0	0.12114	0	0.98846	0
424.837	0	- 0.98846	0	0.12114	0	- 0.08919
- 83.148	0	−0.08651	0	0.16708	0	- 0.982162
- 83.148	- 0.98216	0	0.16708	0	0.08651	0
- 341.689	0	- 0.02883	0	0.98584	0	0.16517
- 341.689	- 0.16517	0	- 0.98584	0	0.02883	0

3.2 Magnetocrystalline Anisotropy Energy:

As was pointed out by Callen and Callen in 1960 [18], the presence of MCA magnetization in a ferromagnet depends upon its orientation as well as upon the temperature. This dependence is depicted in Fig.2, where the variation of E_a with the angles (θ, φ). The varying of $E_a$with θ from 0 to π while φ is fixed to 0 as the variation in the basal plan is insignificant, as seen in Fig.3. It should be noted here that the symmetry reduction to orthorhombic structure is due to a small shift in the position of the as atom, resulting in the preservation of tetragonal symmetry to a large extent, and therefore anisotropy in the basal *ab* - plane is hardly observed.

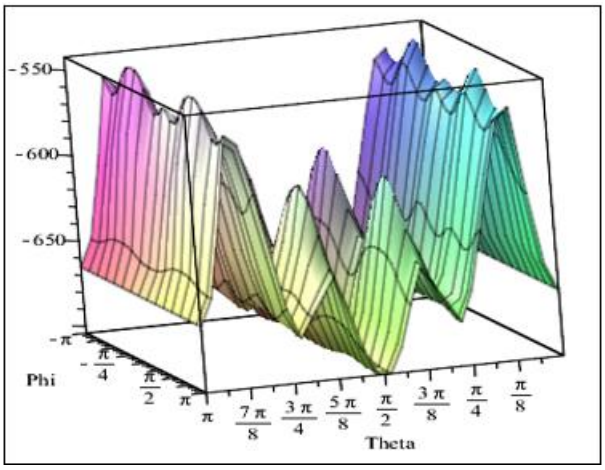

Figure 2: Variation of MAE with directions (θ, φ) with respect to the direction of magnetization (z).

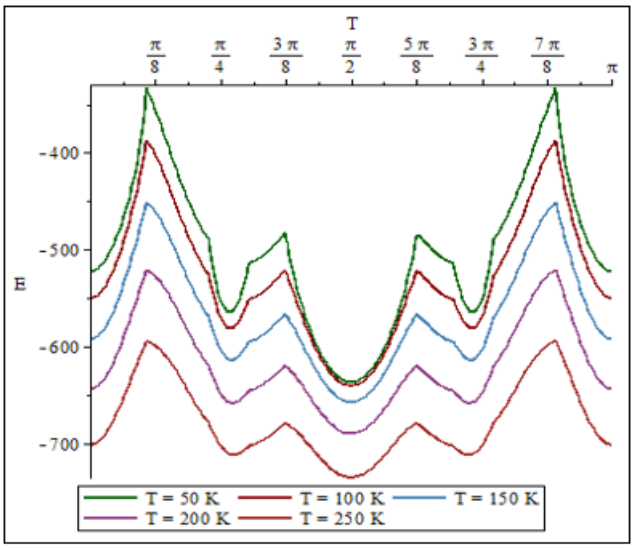

Figure 3: Variation of MAE with the angle θ at different temperatures

Table 3: MAE anisotropy constants K_1 and K_2 at different temperatures.

T [k]	K_1	K_2
5	124.66	- 293.15
50	49.02	- 209.63
100	00.00	- 139.23
150	- 19.59	- 95.97
200	- 25.12	- 69.23
250	- 25.76	- 53.90

In order to estimate the values of anisotropy constants K_1 and K_2 at different temperatures, we have fitted the calculated values as a fourth - order polynomial of direction cosines according to equation (9). Table.3 shows the results of these calculations. Strangely enough, the results show that the leading term K_1 has smaller magnitude than K_2 and that K_2turned to be negative in for all valued in the temperature range considered. The variation of K_1 and K_2 with temperature is depicted in Fig.4.

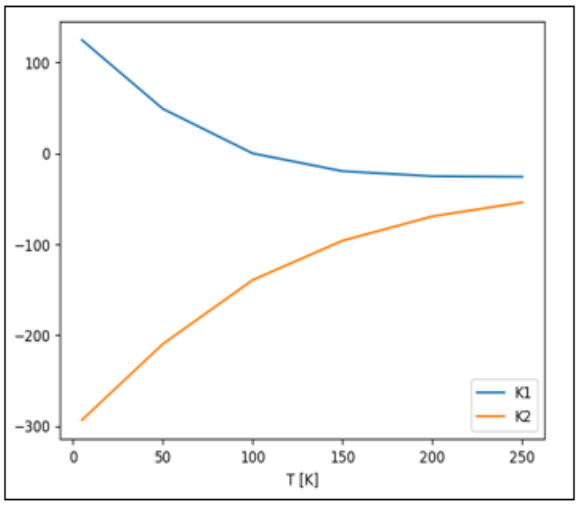

Figure 4: Variation of the anisotropy constants K_1 and K_2 with temperature.

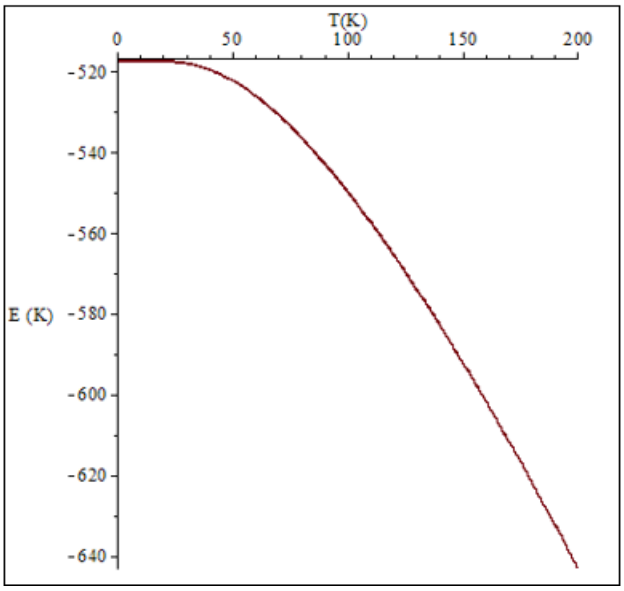

Figure 5: Total free energy as function of temperature for the direction [001].

It is noted here that the absolute value of each of the two parameters is almost exponentially decaying with increasing temperature. This behavior originates from two aspects pertaining to the nature of the model used in the calculation: First, the temperature - dependent term of the effective Hamiltonian, which in this case is the exchange term (H_{ex}), is independent of the site symmetry of the *Ce* ions, so that, regarding the MAE, we expect this term to underlie the temperature dependence of MAE in general, unlike the CF terms, which are mainly due to charge density distribution around the *Ce* ion site.

In conclusion, it is clearly noticed that the magnitude of anisotropy constants and consequently the anisotropy energy (Fig.5) reduces at temperature due to exchange terms rather than CEF. The second reason for MAE to reduce as temperature can be inferred from a physical consideration of the concept of magnetization itself. Since magnetization is attributed to a competitive effect between exchange and thermal effect, it is natural to see a reduction in a major factor leading to spontaneous magnetization (i. e the magnetization energy) ass temperature and the thermal effect is taken as electronic rather than vibrational.

According to Callen and Callen [19, 20], the anisotropy constant K_n for magnetic ions in a crystal environment is given by

$$K_n(T) = K_n(0)\left(\frac{M_s\,(T)}{M_s\,(0)}\right)^{n\,(n+1)\,/2} \qquad (10)$$

where $n = 2$ for K_1 in a uniaxial crystal and $n = 4$ for cubic crystal. For the compound under investigation, Fig.4 clearly shows a qualitative agreement of the temperature variation of K_1 with the Callen and Callen $n\,(n+1)\,/2$ law. The sign of K_1 depends on the RE *4f* charge distribution in the sense that at the lowest order, the MAE can be substituted for the unperturbed Hund's rule ground state $|\psi_{4f}\rangle$ in the CF Hamiltonian [17], so that the anisotropy energy is given by:

$$E_a = \langle\psi_{4f}|V_{CF}|\psi_{4f}\rangle \qquad (11)$$

here the ρ_{4f} is the density given by $\rho_{4f} = \langle\psi_{4f}|\psi_{4f}\rangle$. We can rewrite (11) as follows

$$E_a = \int V_{CF}(\boldsymbol{r})\,\rho_{4f}\,(\boldsymbol{r})\,d\boldsymbol{r} \qquad (12)$$

The electronic charge density $\rho_{4f}\,(\boldsymbol{r})$ has been determined with the aid of Racah algebra as described by Ayuel and de Chatel [21]. The results of our calculations reveal more prolation of the distribution of *4f* - electronic charge density for the case of the Ce^{3+} ion in tetragonal crystal field (Fig.6. a) compared with the case of free Ce^{3+} (Fig.6. b). This result is consistent with the standard calculation based on the superposition model of CF potential [22]. Following the superposition approach for formulating the CF potential, the dipole term of MAE is determined by K_1 given by

$$K_1 = -\tfrac{3}{2}\alpha_J\langle r_{4f}^2\rangle A_2^0\,(3J_z{}^2 - (J(J+1)) \qquad (13)$$

For a fully aligned state $J_z = J$, Eq. (13) reduces to

$$K_1 = -\frac{3}{2}\alpha_J\langle r_{4f}^2\rangle A_2^0\,(2J^2 - J) \qquad (14)$$

where α_J is the second - order Stevens' coefficient, which describes the shape of the ground state *4f* charge density, is determined by Racah fractional parentage method described by Elhag [23]. $\langle r_{4f}^2\rangle$ is the average square of the *4f* - shell radius, and A_2^0 is the second - order CFP that describes the CF potential. A_2^0 is usually obtained by a simple point charge model of CF where neighboring atoms are considered point charges, which produce a multipole expansion of CF potential that interacts with the *4f* - charge density. The prolate or oblate distribution of $\rho_{4f}(\boldsymbol{r})$ results in a positive or negative sign of α_J, respectively [23]. The sign of α_J depends on the 4f count, that is, it takes a negative value for the first three Re ions in each half cycle (i. e., α_J is negative for Ce^{3+}, Pr^{3+}, and Nd^{3+}) [24]. Using equation (A.35) of reference 21, we have obtained $\alpha_J(Ce^{3+}) = -1386$. Furthermore, the *4f* charge distribution shown in Fig.6. b. exhibits an equatorially dented ellipsoid distribution that is oblate. In the case of the Ce ion in CeAgAs2, the 4f shell distribution calculated conforms to the tetragonal distribution of the CF potential, as is clearly seen in Fig 6. a.

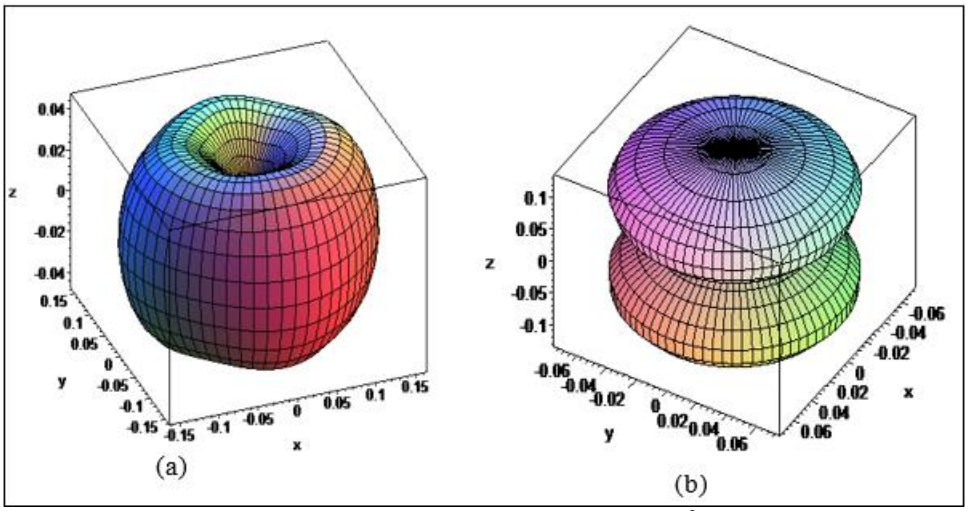

Figure 6. (a) Spatial charge density distribution of *4f* electron shell for Ce^{3+} ion in $CeAgAs_2$. (b) free Ce^{3+} ion

3.3 Magnetization and Magnetic Susceptibility:

The magnetization in the *i*th - direction as per unit cell is given by the average magnetic moments [2].

$$M_i = g_j \mu_B \sum_n \langle n|J_i|n\rangle \frac{e^{-\frac{E_n}{k_B T}}}{Z} \quad (i = x, y. z) \quad (15)$$

The eigenvalues of energy E_n and the corresponding eigenstates $|n\rangle$ are determined by diagonalizing the effective Hamiltonian (1). The hysteresis curve (magnetization vs. applied magnetic field *B*) was calculated for *B* in the range from - 10 to 10 T along the principal crystallographic directions [100], [010], and [001] and temperature T = 2 K. Commensurate with directional variation of MCA, the results depicted in Fig.7 reveal a low response for magnetization in the c - axis compared to ab - plane where the response is identical for both [100] and [010] axes, which is a clear indication that the ab is an easy plane while the c - axis represents the hard direction for magnetization anisotropy. The result is in fairly good agreement with the experimental findings of Mondal et. al. [2], even though their results show the saturation magnetization along [010] - axis is slightly higher than that along the [100] - axis indicating a small anisotropy in the ab plane which is absent in the current investigation. This discrepancy can be explained in view of symmetry considerations, as the unit cell we have theoretically obtained here is a tetragonal (a=b) one which would render a tetragonallysymmetric charge density distributions (Fig.6. a), therefore no in - plane anisotropy is observed.

On the other hand, an orthorhombic crystal structure with a small difference between *a* and *b* was found by Mondal et. al through XRD method. The slight in - plane anisotropy therefore observed may hence be attributed to small variation small difference between *a* and *b*.

The CF magnetic susceptibility was calculated using the equation [25]:

$$\chi_{CF} = N\,(g_J \mu_B)^2 \frac{1}{Z}\left(\sum_{m \neq n} |\langle m|J_i|n\rangle|^2 \frac{1 - e^{-\beta \Delta_{m,n}}}{\Delta_{m,n}} e^{-\beta E_n} + \sum_n \right.$$

where $\beta = \frac{1}{k_B T}$. The results of ${\chi_{CF}}^{-1}$ in the range of T (0–300K) are represented in Fig.8. Upon contrasting Fig.8 with Fig.5, we could notice the consistency of the temperature dependence of magnetic susceptibility with that of MAE. However, it is well understood that either FM or AFM susceptibility originates from MAE; consequently, we should therefore expect such consistency in temperature variation. In comparison with experimental results obtained by magnetometry measurements and represented in Fig.7. a of reference [2], it is apparent that the general trend fairly agrees with experimental measurements for almost the whole range of temperature covered by the investigation except for T < 5 K, where the Neel's temperature is experimentally identified. The inverse molar magnetic susceptibility was also determined by Szlawska et. al. for a tetragonal $CeAgAs_2$ [7]. The results obtained by SQUID magnetometry parallel and perpendicular to [010] direction for temperature range *T (0–400K)* reveals that the compound orders antiferromagnetically with magnetic moment confined to the [010] axis clearly indicating that this direction is the hard one. Referring to the crystallographic axis classification they have adopted, it's worth noting here that the [010] - axis is in fact the c - axis according to our nomenclature. We hence conclude that there is qualitatively good agreement between current results and the results obtained therein.

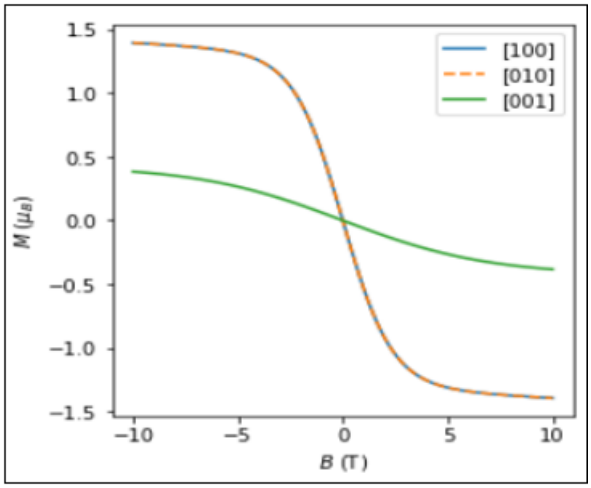

Figure 7: Hysteresis curves for $CeAgAs_2$ at T = 2 K along principal crystallographic axes.

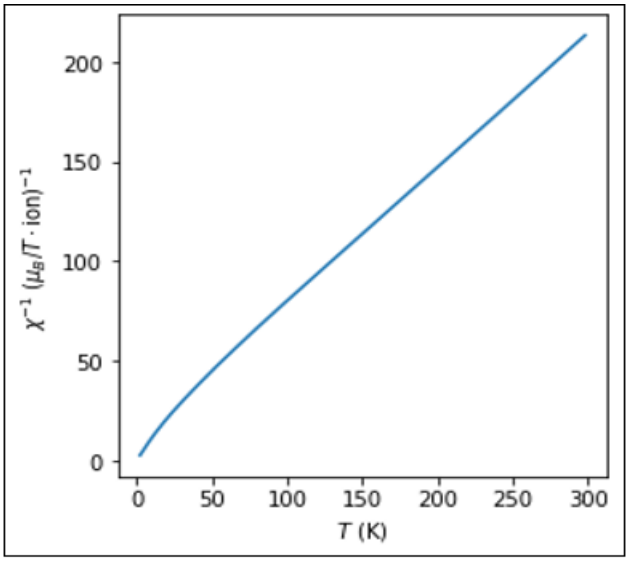

Figure 8: Inverse magnetic susceptibility as a function of temperature.

4. Conclusion

In this study, we have proposed a theoretical model that integrates DFT based ab - initio calculations with CF and mean field approximations to account the magnetocrystalline anisotropies for RE - containing magnetic crystals. The model is used to calculate the effective Hamiltonian and the spatial distribution of charge density, we have subsequently investigated the temperature dependence of the MAE and the magnetic susceptibility as well as the magnetic hysteresis in along the three principal crystallographic axes. The results indicated that, in agreement with previous experimental investigations, $CeAgAs_2$ orders antiferromagnetically and exhibits high magnetic anisotropy with the [001] being the hard axis of magnetization. Moreover, the thermal variation of magnetic susceptibility and the magnetization curve were consistent with experimental findings. The validity of the model seems promising in view of the results obtained for this compound.

Appendix A

We start by considering column matrices $\boldsymbol{O}_k$ and $\boldsymbol{T}_k$of Steven's and Racah tensor operators respectively, then we have the transformation equation for stevens operators O_k^q. according to the transformation [14]:

$$\boldsymbol{O}_k = \boldsymbol{A}_k \cdot \boldsymbol{O}_k \qquad \text{(A1)}$$

Where $\boldsymbol{A}_k$ has only diagonal and antidiagonal non - zero elements. A general transformation for tensor operators is:

$$\{\boldsymbol{T}_k\} = \boldsymbol{D}_k\,[\boldsymbol{T}_k] \qquad \text{(A2)}$$

where $\{\boldsymbol{T}_k\}$ indicate the tensor operators $\hat{T}_k^q$ in the untransformed coordinates and
$[\boldsymbol{T}_k]$ is the transformed tensor.

Using (A1) and (A2), we can transform the operator $\hat{Q}_k^q$ as follows

$$\{\boldsymbol{O}_k\} = \boldsymbol{A}_k \cdot \boldsymbol{D}_k \cdot \boldsymbol{A}_k{}^{-1} \cdot [\boldsymbol{O}_k] = \boldsymbol{S}_k \cdot [\boldsymbol{O}_k] \qquad \text{(A3)}$$

Equation (A3) defines the transformation matrix $\boldsymbol{S}_k\,(\theta, \varphi)$ for a set of Stevens' operators $\hat{Q}_k^q$with a given order k.

References

[1] Z. Fisk, J. L. Sarrao, J. L. Smith, and J. D. Thompson, The physics and chemistry of heavy fermions, Proc. Natl. Acad. Sci. U. S. A.92, 6663, 1995.
[2] R. Mondal, R. Bapat, S. K. Dhar, and A. Thamizhavel, Magnetocrystalline anisotropy in the Kondo - lattice compound $CeAgAs_2$, Phys. Rev.98, 115160, 2018.
[3] K. A. Gshneidner, Jr. and V. K. Pecharsky, Phys. B (Amsterdam, Neth.) 223–224, 131, 1996.
[4] K. D. Myers, S. L. Bud'ko, I. R. Fisher, Z. Islam, H. Kleinke, A. H. Lacerda, and P. C. Canfield, Systematic study of anisotropic transport and magnetic properties of $RAgSb_2$ (R= Y, La - Nd, Sm, Gd - Tm) J. Magn. Magn. Mater.205, 27, 1999.
[5] Demchyna, R. O.; Kuz'ma, Y. B.; Babizhetsky, V. S. New arsenides LnAgAs2 (Ln=La, Ce, Pr, Nd, Sm, Gd, Tb, Dy) and their crystal structure. J. Alloys. Compd., 315, 158, 2001.
[6] Eschen, M.; Jeitschko, W. Preparation and Crystal Structures of Ternary Rare Earth Silver and Gold Arsenides LnAgAs2 and LnAuAs2 with Ln = La - Nd, Sm, Gd, and Tb. Z. Naturforsch., 58, 399–409, 2003.
[7] Szlawska M., Gnida D., Ruszała P., Maciej J., Winiarski, Małgorzata, Schmidt M., Grin Y and Kaczorowski D., Antiferromagnetic Ordering and Transport Anomalies in Single - Crystalline $CeAgAs_2$, Materials, 13, 3865, 2020.
[8] Doert, T.; Schneidewind, A.; Hölzel, M.; Stockert, O.; Rutzinger, D.; Ruck, M. Neutron scattering study on CeAgAs2. J. Magn. Magn. Mater., 324, 1157, 2012.
[9] K. Schwarz, P. Blaha, G. K. H. Madsen. Electronic structure calculations of solids using the WIEN2k package for material sciences. Computer Physics Communications 147 71–76, 2002.
[10] M. Fadila and C. Belkharroubi, Structural, magnetic, electronic and mechanical properties of full - Heusler alloys Co2YAl (Y= Fe, Ti): first principles calculations with different exchange - correlation potentials, Journal of Magnetism and Magnetic Materials, 448, 2018.
[11] Kunes J, Arita R, Wissgott P, Toschi A, Ikeda H and Held K ˇ, Wien2wannier: From linearized augmented plane waves to maximally localized Wannier functions Comput. Phys. Commun.181 1888, 2010.
[12] Mostofi A A, Yates J R, Lee Y S, Souza I, Vanderbilt D and Marzari N, wannier90: A tool for obtaining maximally - localised Wannier functions, Comput. Phys. Commun.178 685, 2008.
[13] Htchigs M. T., Point - Charge Calculations of Energy levels of Magnetic Ions in Crystalline Electric Fields, Solid State Phys., 16, 1964.
[14] Rudowicz, Transformation Relations for the Conventional O_k^q and normalized $\acute{O}_k^q$ Stevens operator equivalents with k = 1 to 6 and - k ≤ q ≤ k, J. Phys. C: Solid State Phys., 181415 - 1430, 1985.
[15] Endichi A., Zaari H., Benyoussef A. and El Kenz A, Structural, electronic and magnetic properties of $LaCr_2Si_2C$: Ab initio calculation, mean field approximation and Monte - Carlo simulation, Results in Physics 9: 1239 - 1245, 2018.

[16] Skomski, R., Manchanda, P., Kashyap, A. Anisotropy and Crystal Field. In: Coey, J. M. D., Parkin, S. S. (eds) Handbook of Magnetism and Magnetic Materials. Springer, Cham, 2021.
[17] Skomski R. and Sellmyer D. J., Anisotropy of rare earth magnets, Journal of rare earths 27, 4: 675, 2009.
[18] Callen E. R. and Callen H. B., Anisotropic Magnetization, J. Phys. Chem. Sol., Vol.16, 310, 1960.
[19] Callen E. R, Temperature dependence of ferromagnetic uniaxial magnetic anisotropy constants, J, Appl. Phys.33: 832, 1962.
[20] Callen H. R. and Callen E, The present status of the temperature dependence of magnetocrystalline anisotropy and the l (l+1) /2 power law, J. Phys. Chem. Solids.27: 1271, 1966.
[21] Ayuel K. and de Chatel P. F, Probability and spin densities of rare earthtri - positive ions, J. Magn. and Magn. Mat.277 43–59, 2004.
[22] Skomski R. and Coey J. M. D., Permanent Magnetism., Bristol Institute of Physics, 1999.
[23] Elhag. A. F. "The Effect of Cubic Crystal Fields on Charge, Spin and Current Densities in Rare Earth Elements", Ph. D thesis, Sudan University of Science and Technology, 2008.
[24] Xu Y., Hongxing L, He B. Cheng Z. and Zi - P. and Zhang W., Electronic Structure and Magnetic Anisotropy of Single - Layer Rare - Earth Oxybromide, ACS Omega, 5, 23, 14194–14201, 2020.
[25] Das K. P., Neeraj Kumar, Kulkarni R, and Thamizhavel A., Magnetic properties of the heavy - fermion antiferromagnet CeMg3, Phys. Rev. B 83, 134416, 2011.